X-ray absorption spectroscopy investigation of the electronic structure of superconducting $FeSe_x$ single crystals

2011 EPL 93 47003

(http://iopscience.iop.org/0295-5075/93/4/47003)

A Letters Journal Exploring the Frontiers of Physics

February 2011

EPL, **93** (2011) 47003
doi: 10.1209/0295-5075/93/47003

www.epljournal.org

X-ray absorption spectroscopy investigation of the electronic structure of superconducting $FeSe_x$ single crystals

C. L. Chen[1(a)], S. M. Rao[1(b)], C. L. Dong[2], J. L. Chen[3,4], T. W. Huang[1], B. H. Mok[1], M. C. Ling[1], W. C. Wang[3], C. L. Chang[3], T. S. Chan[2], J. F. Lee[2], J.-H. Guo[4] and M. K. Wu[1]

[1] *Institute of Physics, Academia Sinica - Taipei 11529, Taiwan*
[2] *National Synchrotron Radiation Research Center - Hsinchu 30076, Taiwan*
[3] *Department of Physics, Tamkang University - Tamsui, Taipei County, Taiwan*
[4] *Advanced Light Source, Lawrence Berkeley National Laboratory - Berkeley, CA 94720, USA*

received 16 September 2010; accepted in final form 21 January 2011
published online 23 February 2011

PACS 78.70.Dm – X-ray absorption spectra
PACS 74.70.Ad – Metals; alloys and binary compounds (including A15, MgB_2, etc.)
PACS 74.25.Jb – Electronic structure (photoemission, etc.)

Abstract – X-ray absorption spectroscopy (XAS) Fe K-edge spectra of the $FeSe_x$ ($x = 1$–0.8) single crystals cleaved *in situ* under vacuum reveal characteristic Fe $4sp$ states and a lattice distortion. The Se K-edge spectra point to a strong Fe $3d$-Se $4p$ hybridization giving rise to itinerant charge carriers. A formal charge of $\sim$1.8+ for Fe and $\sim$2.2− for Se was evaluated from these spectra in the $FeSe_x$ ($x = 0.88$). The charge balance between Fe and Se is assigned to itinerant electrons located in the Fe-Se hybridization bond. As x decreases the $4p$ hole count increases and a crystal structure distortion is observed that in turn causes the Fe separation in the ab-plane change from $4p$ orbital to varying (modulating) coordination. Powder X-ray diffraction (XRD) measurements also show a slight increase in lattice parameters as x decreases (increasing Se deficiency).

Introduction. – Recent report of superconductivity in oxypnictides [1–3] has generated a flurry of activity much akin to the cuprate superconductivity discovered in the 1980s. This has led to the discovery of several new compounds among which is the less toxic $FeSe_x$ [4] that shows zero resistance at 8 K which is dependent on Se deficiency and annealing at 400 ℃. While the 400 ℃ anneal is found to reduce the non-superconducting NiAs-type hexagonal phase and increase the PbO-type tetragonal superconducting phase [4–6] the role of Se deficiency is not well understood. On the other hand, the influence of fluorine doping [1,7] and rare-earth substitutions [8] on the superconductivity in the $LaO_{1-x}F_xFeAs$ compounds have been investigated. The XAS [9], X-ray photoemission spectroscopy (XPS) [10] and resonant X-ray inelastic scattering (RIXS) [8] investigations show that the Fe $3d$ states hybridize with the As $4p$ states providing the itinerant charge carriers (electrons) responsible for superconductivity. Most of these studies suggest moderate-to-weak electronic correlations in this system. The photoemission spectroscopy (PES) measurements [11] support the density of state (DOS) calculations on the $FeSe_x$ system and indicate the Fe-Se hybridization and itinerancy with weak-to-moderate electronic correlations [12] while strong correlations have been suggested is some recent theoretical calculations [13,14]. While fluorine substitution leads to electron doping in case of the $LaO_{1-x}F_xFeAs$ system, how Se deficiency may bring in the mobile carriers in the $FeSe_x$ system leading to superconductivity is not clear. A detailed study of the $FeSe_x$ ($x = 1$–0.8) crystals has been made using XAS Fe and Se K-edge spectra. The results presented here show a lattice distortion and Fe-Se hybridization that are probably responsible for producing itinerant charge carriers in this system. The lattice distortion was also confirmed by the powder X-ray diffraction (XRD) measurements.

Experimental. – $FeSe_x$ crystals were grown by the high-temperature solution method as described earlier [5,6]. Crystals measuring 5 mm × 5 mm × 0.2 mm with (101) plate-like habit thus obtained were characterized for Se deficiency using a Philips Xpert XRD system and a Joel scanning electron microscope (SEM) coupled with an energy dispersive X-ray spectrometer (EDS) (not presented here). The XAS measurements

(a) E-mail: clchen@phys.sinica.edu.tw
(b) E-mail: rao@phys.sinica.edu.tw

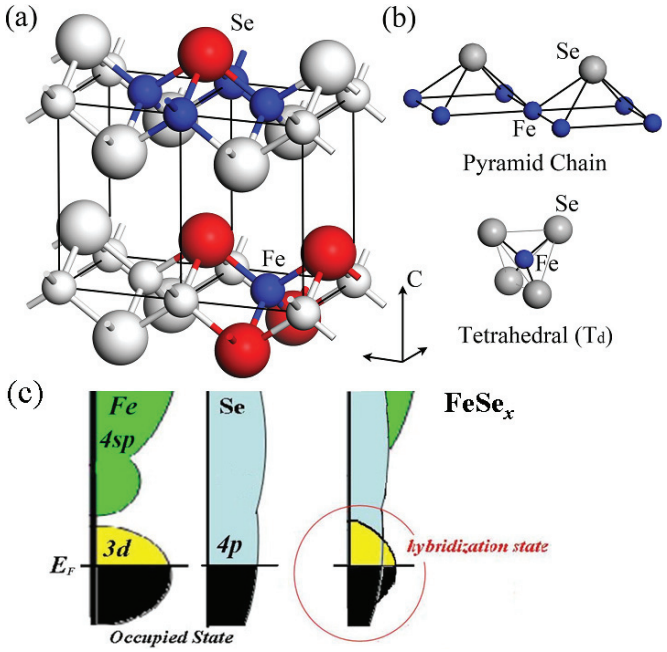

Fig. 1: (Color online) (a) Illustration of the crystal structure of tetragonal $FeSe_x$, the blue (small balls) and red (large balls) denote Fe and Se, respectively; the pyramid chain and tetrahedral arrangements are marked in color in the unit cell. The hybridization is shown in two color bonds; (b) the local symmetry of Se atom in pyramid chain and Se atom in tetrahedral geometry shown separately; (c) energy level diagram of the $FeSe_x$ system along with the individual elements. The hybridization and unoccupied states in the FeSe are highlighted by a circle.

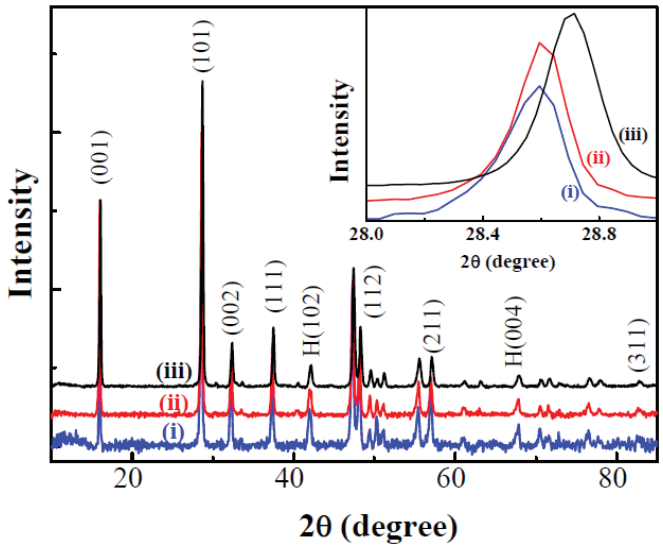

Fig. 2: (Color online) Powder XRD patterns of $FeSe_x$ crystals with $x = 0.85$ (i), 0.88 (ii) and 0.9 (iii). The patterns are fitted to the $P4/nmm$ space group and indexed. The hexagonal phase reflections are marked with a prefix H.

at the Fe and Se K-edge were carried out on the 17C1 and 01C Wiggler beamlines at the National Synchrotron Radiation Reach Center (NSRRC) in Taiwan, operated at 1.5 GeV with a current of 200–240 mA. Si (111) crystals monochromators were used on both the beam lines giving an energy resolution $\Delta E/E$ better than 2×10^{-4}. The Fe and Se K-edge absorption spectra were recorded by the fluorescence yield (FY) mode at room temperature using a Lytel detector [15]. All spectra were normalized to a unity step height in the absorption coefficient from well below to well above the edges. Standard Fe and Se metal foils and oxide powders, SeO_2, FeO, Fe_2O_3 and Fe_3O_4 were used for energy calibration and also for comparing different electronic valence states. Since surface oxidation was suspected the FeSe crystals were cleaved *in situ* in vacuum before recording the spectra. Even though we have studied a number of $FeSe_x$ crystals with $x = 1$ to 0.8 the results for only three compositions are presented here for comparison and clarity.

Results and discussion. –

Microstructure. To facilitate the discussion that follows the tetragonal crystal structure of FeSe and its building blocks, namely, Se-Fe tetrahedra and Fe-Se pyramidal sheets are shown in fig. 1(a). The electronic structure of the individual elements and $FeSe_x$ (indicating the hybridization band) are given in fig. 1(b). Figure 2 shows the XRD patterns of the $FeSe_x$ ($x = 0.9$, 0.88 and 0.85) crystals which are found to represent the superconducting FeSe phase. The patterns have been fitted to the $P4/nmm$ and indexed in the figure. Weak hexagonal reflections are also seen among these. The main diffraction peak (101) shown expanded in the inset is found to shift to a lower 2θ as x decreases indicating an increase in the lattice parameters. The lattice parameters calculated from these patterns are $a = b = 3.771$ Å, $c = 5.528$ Å for $x = 0.9$, $a = b = 3.775$ Å, $c = 5.528$ Å for $x = 0.88$ and $a = b = 3.777$ Å, $c = 5.529$ Å for $x = 0.85$. It is observed that the $a = b$ parameter increases though very slightly as x decreases. A much smaller change is seen in the c-parameter at the same time. Thus, the ab-plane variation is found to be larger than that of the c-axis. These lattice parameters are very close to those reported in literature for Se-deficient powders [4].

Formal charge of Fe and Se in the crystals. The transition metal Fe K-edge ($1s \rightarrow 4p$) XAS spectra in fig. 3(a) are mostly related to the partial density of $4p$ states of the iron site (fig. 1(c)). The unoccupied states in the $3d$ (due to quadruple transition) and $4sp$ bands are sensitive to the local structure and the type of nearest neighbors [16–18] These spectra could therefore be used to obtain information about the changes in the electronic states that may result from changes in the environment of the Fe ions such as Se vacancies in the present case. The Fe K-edge absorption spectra of $FeSe_x$ crystals are presented in fig. 3 along with the standards Fe, FeO, Fe_2O_3 and Fe_3O_4 and are normalized for the photon energy ∼100 eV above the absorption edge at $E_0 = 7112$ eV (the pure Fe K absorption edge energy). The spectra of the crystals appear to

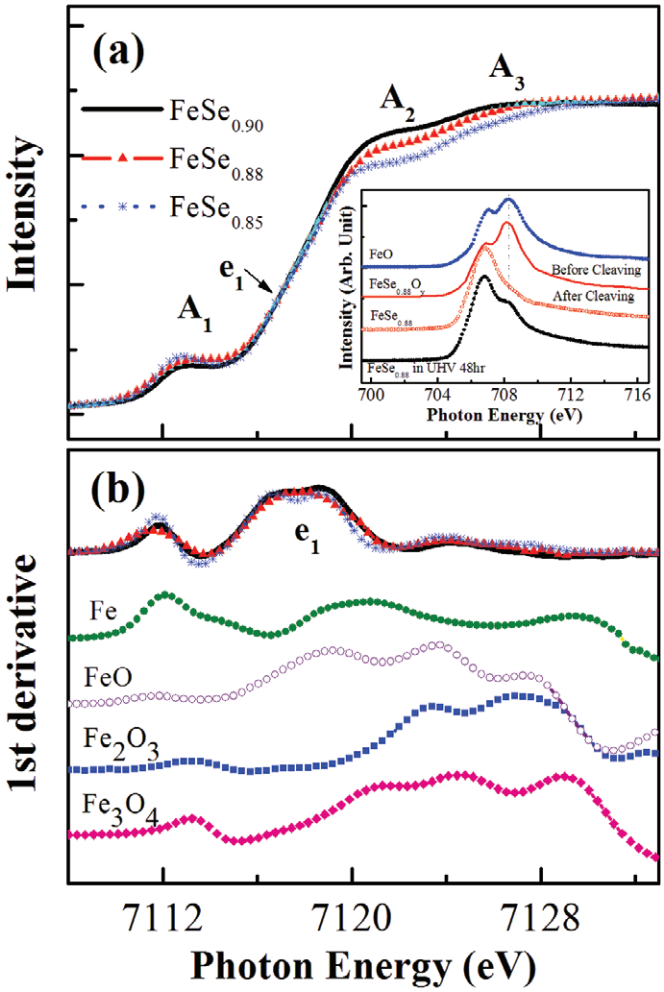

Fig. 3: (Color online) (a) Fe K-edge ($1s \to 4p$) absorption spectra of $FeSe_x$ with different Se content and the inset is shown the XAS Fe L_3-edge spectra of the $FeSe_{0.88}$ crystal before and after cleaving *in situ* in vacuum; (b) the first-derivative plots of the same spectra. The spectra of the standards Fe metal foil, FeO, Fe_2O_3 and Fe_3O_4 are also given alongside the sample spectra.

be close to the Fe metal foil indicating that the crystals are free from oxidation. This was further confirmed from the recent Fe L-edge ($2p_{2/3} \to 3d$ transition) spectra measured before and after cleaving the samples in UHV, as shown in the inset of fig. 3(a). The oxidation peak observed in the crystal before cleaving is not observed after cleaving indicating the possible formation of a thin oxide layer on the surface during handling. Such thin layer may not have much impact on the deeper penetrating K-edge measurements. Since our measurements were made after cleaving the crystals under vacuum even this possibility is eliminated. The spectral line shapes of the cleaved crystals resemble those of ion metal suggesting a strong covalent bounding in the interlayers of the Fe plane. More details about the $FeSe_x$ electronic structure of the $3d$ states obtained by XAS measurements and resonant inelastic X-ray scattering (RIXS) at the Fe $L_{2,3}$-edges will be discussed separately [19]. Our observations are in agreement with the results of Yang *et al.* [8] on Fe-pnictides 1111 and 122 systems and Lee *et al.* [20] using first-principles methods to study the $FeSe_x$ system. Thus the results presented here on the oxygen-free $FeSe_x$ crystals rule out the role of oxygen in superconductivity as is the case in the $LaO_{1-x}F_xFeAs$ system.

Three prominent features A_1, A_2 and A_3 are observed in these spectra (fig. 3(a)) of which the A_1 could be assigned to the $3d$ unoccupied states originating from the Fe-Fe bonds in metallic iron. The features A_2 and A_3 represent the unoccupied Fe $4sp$ states. The rising part of the broad feature A_2 (∼7118.8 eV) appears as a broad peak labeled e_1 at ∼7116.8 eV, seen well separated in the first-derivative plots of these spectra given in fig. 3(b). It is not seen in those of the reference Fe metal foil or oxide powders and is a part of the Fe $4sp$ band. The e_1 feature appears at an energy between those of the Fe metal and FeO and therefore has its origin in a different interaction as will be seen. From these first-derivative plots, a formal charge of Fe was evaluated in conjunction with the three standards $FeO(Fe^{2+})$, $Fe_2O_3(Fe^{3+})$ and $Fe_3O_4(Fe^{2.66+})$. In addition we used the sine-function fitting of the broad feature e_1 (7113.84–7122.2 eV). By an extrapolation of the energy of $FeSe_{0.88}$ with those of the standards we obtained a formal charge of ∼1.8+ for Fe in these crystals thus establishing the electronic charge of Fe in the covalency (2+). It is also seen that the peak (energy) position is not increasing in energy as x is decreased meaning that the effective charge (valence) of Fe does not change with x. This is consistant with the Fe L-edge spectra presented above as well as the RIXS analysis [19]. Thus the possible electronic configurations of Fe in the ground state could be written as $3d^{6.2}$ or $3d^6 4s^{0.2}$ indicating a mixture of monovalency ($3d^6 4s^1$ or $3d^7$) and divalency ($3d^6$).

The Se K-edge spectra of the $FeSe_x$ crystals and Se and SeO_2 standards are presented in fig. 4(a) and the corresponding first-derivative plots are given in fig. 4(b) to highlight the energy changes in the spectra. The spectra represent mainly Se character without any trace of SeO_2, indicating the absence of oxidation even in the deeper layers of the $FeSe_x$ crystals. The spectra exhibit two peaks B_1 and B_2. The B_1 feature at photon energy around 12658 eV is formally assigned to the transitions $1s \to 4p$ and shows a slight increase in intensity as well as shift to higher energy as x is decreased. This indicates an increase in the Se $4p$ unoccupied states *i.e.* in the upper Hubbard band (UHB). From the first-derivative plots a formal charge of ∼2.2− is obtained for Se in the $x = 0.88$ crystal by interpolation with the energies of the standards Se and SeO_2 (as in the case of Fe). This is in agreement with a total charge of 0 when the formal charges of Fe and Se are added ($Fe^{1.8+}$ $Se^{2.2-}_{0.88}$). This establishes the electronic charge of Se in the covalency (2−).

Fe 3d-Se 4p hybridization and superconductivity. The excess negative charge of −0.2 seen on Se may be explained as follows. The electronic charge of Fe in the

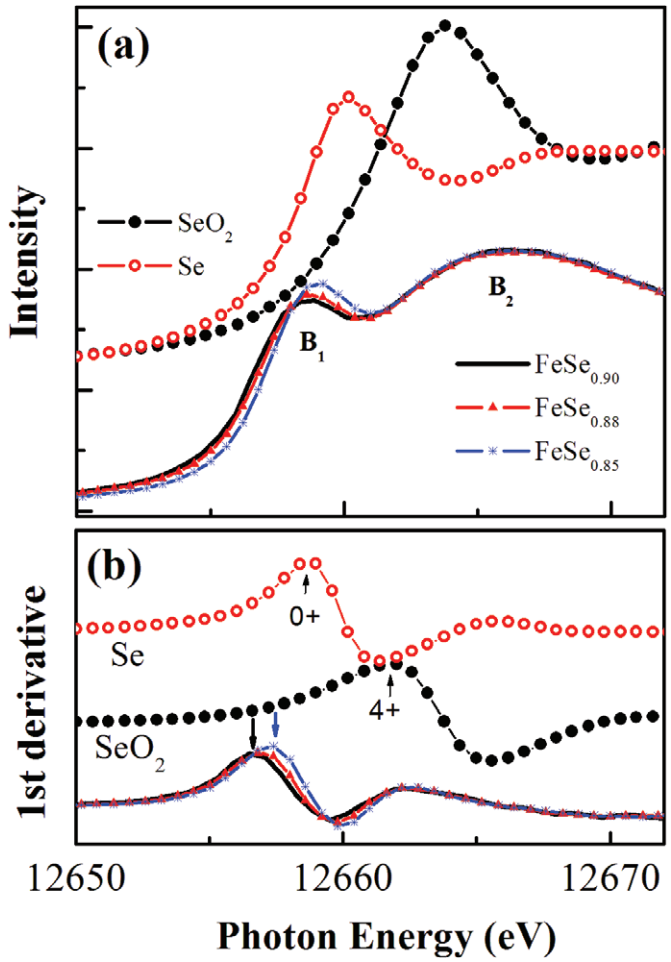

Fig. 4: (Color online) (a) The Se K-edge ($1s \rightarrow 4p$) absorption spectra $FeSe_x$ with different Se content along with the standards Se metal and SeO_2 and (b) the first-derivative plots of the same spectra.

covalent $FeSe_x$ should be 2+. However we have obtained a formal charge of 1.8+ which means that some electronic charge is returned to Fe due to the Se deficiency. On the other hand the covalent charge of Se should be 2− but we obtain 2.2−, which is beyond the 6 electron occupancy of the $4p$ state orbitals. A hole increase is seen from the Se K-edge spectra as x decreases but no change is observed in the Fe K-edge to suggest a change in valence. The close distance between Se and Fe, might result in an increase in the covalence of the Fe-Se bond due to the hybridization of Se $4p$ and Fe $3d$ states as pointed by Yamasaki *et al.* [11] from their soft-X-ray photoemission spectroscopy (XPS) measurements. Yoshida *et al.* [12] also observe a good correspondence between their DOS calculations and the XPS spectra which show a feature corresponding to the Fe $3d$-Se $4p$ hybridization. Theoretical calculation by Subedi *et al.* [21] also point to this Fe-Se hybridization. From the discussion above, it may be concluded that the B_1 feature (fig. 4(a)) represents the Fe $3d$-Se $4p$ hybridization band (fig. 1(c)) and the increased electronic charge on Fe seen above is in fact due to itinerant electrons in the Fe-Se hybridization bond and appears as a hole increase in the Se K-edge spectra. This could be confirmed from the Fe L-edge measurements on similar crystals. When we correlate this with the decreasing transition width in the resistance measurements (not shown here), it becomes apparent that that the charge carriers responsible for superconductivity are in fact itinerant electrons in a similar manner as the itinerant holes in the case of cuprates. Oxygen annealing in case of $YBa_2Cu_3O_{6+\delta}$, is found to oxidize Cu^{2+} to Cu^{3+} through the hybridization of Cu $3d$-O $2p$ states. The Cu^{3+} state has been assigned to the empty state in the Cu-O bonds that is also referred to as the $3d^9\underline{L}$ ligand state, where a hole is located in the oxygen ions surrounding a "Cu site" ($\underline{L}$, a ligand hole, tentatively label this as $3d^8$-like) [22]. These itinerant holes are responsible for superconductivity. In a similar manner in the case of $FeSe_x$, the Se deficiency is bringing a Fe $3d$-Se $4p$ hybridization leading to itinerant electrons. It is also likely that the changes in bond lengths may also result in a reduction in the width of the resistive transition due to external pressure as reported by Mizuguchi *et al.* [23].

Lattice distortion, structure modulation. It is seen that the intensity of the A_2 feature reduces as x is decreased which indicates a lattice distortion that increases with decreasing x. In addition the change in the A_2 feature is larger than the A_3 feature. Since multiple scattering in the XAS from p-orbitals could reveal the different orbital orientations and because of the nature of the p-orbitals *i.e.* p_{xy} and p_z the A_2 feature could be associated with $p_{xy}(\sigma)$ and A_3 to $p_z(\pi)$ orientations. This leads us to a speculation of a larger distortion in the ab-plane (Fe-Fe distance) compared to the c-axis. This is also seen from the XRD measurements (fig. 2) where the change in the $a = b$ parameter is larger than that of the c-parameter (Fe-Se distance). Therefore, the Fe orbital structure changes from $4p$ to a varying (modulating) coordination as x is decreased. The broad feature B_2, at $\sim$20 eV above the Se K-edge appears at the same energy in all the $FeSe_x$ spectra and is not affected by the Se deficiency and is assigned to the multiple scattering from the symmetrical Se $4p$ states in the coordination sphere that are correlated to the local structure of the Se ions [16]. This is consistent with the XRD result where the c-parameter is nearly unchanged. This becomes clear by looking at fig. 1 where Se is seen at the tip of the Fe-Se pyramid.

Since Se is located at the apex of the tetrahedral pyramid chain in the $FeSe_x$ lattice (as shown in fig. 1), the removal of a Se ion with formal negative charge (−2) from the lattice would result in a Se vacancy with an effective positive charge and would cause repulsion to the surrounding positively charged Fe atoms. This is consistent with the distortion in the ab-plane discussed above. In addition the Fe atoms around the vacancy may act like magnetic clusters as pointed out by Lee *et al.* [20].

Conclusion. – In conclusion a lattice distortion observed in the XAS Fe K-edge spectra of Se-deficient $FeSe_x$ crystals that may produce itinerant electrons in the Fe-Se hybridization bond seen in the Se K-edge spectra. The XRD measurements confirm this lattice distortion that increases with Se deficiency. The charge balance considerations from Se deficiency also result in itinerant electrons (in the Fe-Se hybridization bond). The increase in x (itinerant electrons) is ascribed to the reduced width of the resistive (superconducting) transition. The symmetry of the Fe in the ab-plane changes from the $4p$ orbital to modulating (varying) coordination geometry.

* * *

This work was supported by the National Science Council of R. O. C. under contracts NSC96-2112-M-001-026-MY3 and NSC 99-2112-M-001-036-MY3. One of the authors (SMR) is grateful to the NSC for financial support. The experimental support from NSRRC is gratefully acknowledged.

REFERENCES

[1] Kamihara Y., Watanabe T., Hirano M. and Hosono H., *J. Am. Chem. Soc.*, **130** (2008) 3296.

[2] Takahashi H., Igawa K., Arii K., Kamihara Y., Hirano M. and Hosono H., *Nature* (London), **453** (2008) 376.

[3] Ren Z.-A., Lu W., Yang J., Yi W., Shen X.-L., Li Z.-C., Che G.-C., Dong X.-L., Sun L.-L., Zhou F. and Zhao Z.-X., arXiv:0804.2053 (2008).

[4] Hsu F. C., Luo J. Y., Yeh K. W., Chen T. K., Huang T. W., Wu P. M., Lee Y. C., Huang Y. L., Chu Y. Y., Yan D. C. and Wu M. K., *Proc. Natl. Acad. Sci. U.S.A.*, **105** (2008) 14262.

[5] Wu M. K., Hsu F. C., Yeh K. W., Huang T. W., Luo J. Y., Wang M. J., Chang H. H., Chen T. K., Rao S. M., Mok B. H., Chen C. L., Huang Y. L., Ke C. T., Wu P. M., Chang A. M., Wu C. T. and Perng T. P., *Physica C*, **469** (2009) 9; 340.

[6] Mok B. H., Rao S. M., Ling M. C., Wang K. J., Ke C. T., Wu P. M., Chen C. L., Hsu F. C., Huang T. W., Luo J. Y., Yan D. C., Yeh K. W., Wu T. B., Chang A. M. and Wu M. K., *Cryst. Growth Des.*, **9** (2009) 3260.

[7] Dong J., Zhang H. J., Xu G., Li Z., Li G., Hu W. Z., Wu D., Chen G. F., Dai X., Luo J. L., Fang Z. and Wang N. L., *EPL*, **83** (2008) 27006.

[8] Yang W. L., Sorini A. P., Chen C.-C., Moritz B., Lee W.-S., Vernay F., Olalde-Velasco P., Denlinger J. D., Delley B., Chu J.-H., Analytis J. G., Fisher I. R., Ren Z. A., Yang J., Lu W., Zhao Z. X., van den Brink J., Hussain Z., Shen Z.-X. and Devereaux T. P., *Phys. Rev. B*, **80** (2009) 014508.

[9] Kroll T., Bonhommeau S., Kachel T., Dürr H. A., Werner J., Behr G., Koitzsch A., Hübel R., Leger S., Schönfelder R., Ariffin A. K., Manzke R., de Groot F. M. F., Fink J., Eschrig H., Büchner B. and Knupfer M., *Phys. Rev B*, **78** (2008) 220502.

[10] Malaeb W., Yoshida T., Kataoka T., Atsushi Fujimori A., Kubota M., Ono K., Usui H., Kuroki K., Arita R. and Hosono H., *J. Phys. Soc. Jpn.*, **77** (2008) 093714.

[11] Yamasaki A., Matsui Y., Imada S., Takase K., Azuma H., Muro T., Kato Y., Higashiya A., Sekiyama A., Suga S., Yabashi M., Tamasaku K., Ishikawa T., Terashima K., Kobori H., Sugimura A., Umeyama N., Sato H., Hara Y., Miyagawa N. and Ikeda I., *Phys. Rev. B*, **82** (2010) 184511.

[12] Yoshida R., Wakita T., Okazaki H., Mizuguchi Y., Tsuda S., Takano Y., Takeya H., Hirata K., Muro T., Okawa M., Ishizaka K., Shin S., Harima H., Hirai M., Muraoka Y. and Yokoya T., *J. Phys. Soc. Jpn.*, **78** (2009) 034708.

[13] Aichhorn M., Biermann S., Miyake T., Antoine Georges A. and Masatoshi Imada M., *Phys. Rev. B*, **82** (2010) 064504.

[14] Pourret A., Malone L., Antunes A. B., Yadav C. S., Paulose P. L., Fauqué B. and Behnia K., arXiv:1010.1484v2 [cond-mat.supr.-con] (2010).

[15] Lytle F. W., Greegor R. B., Sandstrom D. R., Marques E. C., Wong J., Spiro C. L., Huffman G. P. and Huggins F. E., *Nucl. Instrum. Methods*, **226** (1984) 542.

[16] de Groot F., Vankó G. and Glatzel P., *J. Phys.: Condens. Matter*, **21** (2009) 104207.

[17] Chang C. L., Chen C. L., Dong C. L., Chern G., Lee J.-F. and Jang L. Y., *J. Electron Spectrosc. Relat. Phenom.*, **114** (2001) 545.

[18] Longa S. D., Arcovito A., Vallone B., Castellano A. C., Kahn R., Vicat J., Soldo Y. and Hazemann J. L., *J. Synchrotron Radiat.*, **6** (1999) 1138.

[19] Chen C. L., Dong C. L., Chen J. L., Guo J-H., Yang W. L., Yeh K. W., Huang T. W., Mok B. H., Chan T. S., Chang C. L., Rao S. M. and Wu M. K., *The investigation of the electronic states in $FeSe_x$ single crystals and FeSe doped with Te by XAS and RIXS* (unpublished).

[20] Lee K.-W., Pardo V. and Pickett W. E., *Phys. Rev. B*, **78** (2008) 174502.

[21] Subedi A., Zhang L., Singh D. J. and Du M. H., *Phys. Rev. B*, **78** (2008) 134514.

[22] Grioni M., Goedkoop J. B., Schoorl R., de Groot F. M. F., Fuggle J. C., Schäfers F., Koch E. E., Rossi G., Esteva J.-M. and Karnatak R. C., *Phys. Rev. B*, **39** (1989) 1541; Merz M., Nücker N., Schweiss P., Schuppler S., Chen C. T., Chakarian V., Freeland J., Idzerda Y. U., Kläser M., Müller-Vogt G. and Wolf Th., *Phys. Rev. Lett.*, **80** (1998) 5192.

[23] Mizuguchi Y., Tomioka F., Tsuda S., Yamaguchi T. and Takano Y., *Appl. Phys. Lett.*, **93** (2008) 152505.